研究成果の刊行に関する一覧表

書籍

著者氏名	論文タイトル名	書籍全体の編集者名	書　籍　名	出版社名	出版地	出版年	ページ
植田幸嗣	プロテオーム解析から見たバイオマーカーとしてのエクソソームとその特徴	落谷孝広	細胞工学 vol.32 No.1	株式会社学研メディカル秀潤社	日本	2013年	8
植田幸嗣	新規血清マーカー	有井滋樹	肝胆膵第66巻2号	株式会社アークメディア	日本	2013年	7

雑誌

発表者氏名	論文タイトル名	発表誌名	巻号	ページ	出版年
G. Toyokawa, M. Yoshimatsu, M. Nakakido, V. Saloura, K. Sone, L. Piao, H. S. Cho, K. Ueda, Y. Maehara, Y. Nakamura, and R. Hamamoto	SMYD2-dependent HSP90 methylation promotes cancer cell proliferation by regulating the chaperonin complex formation.	Cancer letters	In press	In press	2014
T. Fujitomo, Y. Daigo, K. Matsuda, K. Ueda, and Y. Nakamura	Identification of a nuclear protein, LRRC42, involved in lung carcinogenesis.	International journal of oncology	45 (1)	147-56	2014

M. Unoki, A. Masuda, N. Dohmae, K. Arita, M. Yoshimatsu, Y. Iwai, Y. Fukui, K. Ueda, R. Hamamoto, M. Shirakawa, H. Sasaki, and Y. Nakamura	Lysyl 5-Hydroxylation, a Novel Histone Modification, by Jumonji Domain Containing 6 (JMJD6).	The Journal of biological chemistry	288 (9)	6053-62	2013
K. Ueda, A. Tatsuguchi, N. Saichi, A. Toyama, K. Tamura, M. Furihata, R. Takata, S. Akamatsu, M. Igarashi, M. Nakayama, T. A. Sato, O. Ogawa, T. Fujioka, T. Shuin, Y. Nakamura, and H. Nakagawa	Plasma Low-Molecular-Weigh t Proteome Profiling Identified Neuropeptide-Y as a Prostate Cancer Biomarker Polypeptide.	Journal of proteome research	12 (10)	4497-506	2013
K. Ueda	Glycoproteomic strategies: from discovery to clinical application of cancer carbohydrate biomarkers.	Proteomics Clin Appl	7 (9-10)	607-17	2013

M. Ishihara, N. Araya, T. Sato, A. Tatsuguchi, N. Saichi, A. Utsunomiya, Y. Nakamura, H. Nakagawa, Y. Yamano, and K. Ueda	Preapoptotic protease calpain-2 is frequently suppressed in adult T-cell leukemia.	Blood	121 (21)	4340-7	2013
M. Kogure, M. Takawa, V. Saloura, K. Sone, L. Piao, K. Ueda, R. Ibrahim, T. Tsunoda, M. Sugiyama, Y. Atomi, Y. Nakamura, and R. Hamamoto	The oncogenic polycomb histone methyltransferase EZH2 methylates lysine 120 on histone H2B and competes ubiquitination.	Neoplasia	15(11)	1251-61	2013
A. Toyama, H. Nakagawa, K. Matsuda, T. A. Sato, Y. Nakamura, and K. Ueda	Quantitative structural characterization of local N-glycan microheterogeneity in therapeutic antibodies by energy-resolved oxonium ion monitoring.	Analytical chemistry	84(22)	9655-62	2012

C. Tanikawa, M. Espinosa, A. Suzuki, K. Masuda, K. Yamamoto, E. Tsuchiya, K. Ueda, Y. Daigo, Y. Nakamura, and K. Matsuda	Regulation of histone modification and chromatin structure by the p53-PADI4 pathway.	Nature communications	3	676	2012
M. Takawa, H. S. Cho, S. Hayami, G. Toyokawa, M. Kogure, Y. Yamane, Y. Iwai, K. Maejima, K. Ueda, A. Masuda, N. Dohmae, H. I. Field, T. Tsunoda, T. Kobayashi, T. Akasu, M. Sugiyama, S. Ohnuma, Y. Atomi, B. A. Ponder, Y. Nakamura, and R. Hamamoto	Histone lysine methyltransferase SETD8 promotes carcinogenesis by deregulating PCNA expression.	Cancer research	72(13)	3217-27	2012
M. H. Nguyen, K. Ueda, Y. Nakamura, and Y. Daigo	Identification of a novel oncogene, MMS22L, involved in lung and esophageal carcinogenesis.	International journal of oncology	41(4)	1285-96	2012

T. Fujitomo, Y. Daigo, K. Matsuda, K. Ueda, and Y. Nakamura	Critical function for nuclear envelope protein TMEM209 in human pulmonary carcinogenesis.	Cancer research	72(16)	4110-8	2012
S. Chung, H. Suzuki, T. Miyamoto, N. Takamatsu, A. Tatsuguchi, K. Ueda, K. Kijima, Y. Nakamura, and Y. Matsuo	Development of an orally-administrative MELK-targeting inhibitor that suppresses the growth of various types of human cancer.	Oncotarget	3(12)	1629-40	2012
K. Ueda, N. Saichi, S. Takami, D. Kang, A. Toyama, Y. Daigo, N. Ishikawa, N. Kohno, K. Tamura, T. Shuin, M. Nakayama, T. A. Sato, Y. Nakamura, and H. Nakagawa	A comprehensive peptidome profiling technology for the identification of early detection biomarkers for lung adenocarcinoma.	PLoS One	6(4)	e18567	2011

A. Toyama, H. Nakagawa, K. Matsuda, N. Ishikawa, N. Kohno, Y. Daigo, T. A. Sato, Y. Nakamura, and K. Ueda	Deglycosylation and label-free quantitative LC-MALDI MS applied to efficient serum biomarker discovery of lung cancer.	Proteome Sci	9	18	2011
L. Piao, H. Nakagawa, K. Ueda, S. Chung, K. Kashiwaya, H. Eguchi, H. Ohigashi, O. Ishikawa, Y. Daigo, K. Matsuda, and Y. Nakamura	C12orf48, termed PARP-1 binding protein, enhances poly(ADP-ribose) polymerase-1 (PARP-1) activity and protects pancreatic cancer cells from DNA damage.	Genes Chromosomes Cancer	50(1)	13-24	2011

Enzymology:

Lysyl 5-Hydroxylation, a Novel Histone Modification, by Jumonji Domain Containing 6 (JMJD6)

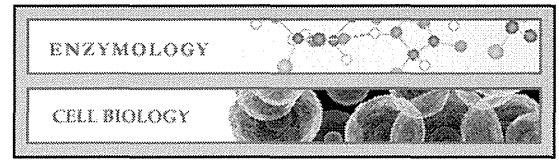

Motoko Unoki, Akiko Masuda, Naoshi Dohmae, Kyohei Arita, Masanori Yoshimatsu, Yukiko Iwai, Yoshinori Fukui, Koji Ueda, Ryuji Hamamoto, Masahiro Shirakawa, Hiroyuki Sasaki and Yusuke Nakamura

J. Biol. Chem. 2013, 288:6053-6062.
doi: 10.1074/jbc.M112.433284 originally published online January 9, 2013

THE JOURNAL OF BIOLOGICAL CHEMISTRY VOL. 288, NO. 9, pp. 6053–6062, March 1, 2013

Lysyl 5-Hydroxylation, a Novel Histone Modification, by Jumonji Domain Containing 6 (JMJD6)*

Received for publication, November 3, 2012, and in revised form, January 8, 2013 Published, JBC Papers in Press, January 9, 2013, DOI 10.1074/jbc.M112.433284

Motoko Unoki[‡§1], Akiko Masuda[¶], Naoshi Dohmae[¶], Kyohei Arita[‖], Masanori Yoshimatsu[**], Yukiko Iwai[‡‡], Yoshinori Fukui[‡‡], Koji Ueda[§], Ryuji Hamamoto[§§], Masahiro Shirakawa[**], Hiroyuki Sasaki[‡], and Yusuke Nakamura[**§§]**

From the [‡]Division of Epigenetics, Department of Molecular Genetics, Medical Institute of Bioregulation, Kyushu University, Fukuoka 812-8582, Japan, the [§]Laboratory for Biomarker Development, The Institute of Physical and Chemical Research, Center for Genomic Medicine, RIKEN, Tokyo 108-8639, Japan, the [¶]Biomolecular Characterization Team, RIKEN, Saitama 351-0198, Japan, the [‖]Graduate School of Engineering, Kyoto University, Kyoto 615-8510, Japan, the [**]Laboratory of Molecular Medicine, Human Genome Center, Institute of Medical Science, The University of Tokyo, Tokyo 108-8639, Japan, the [‡‡]Division of Immunogenetics, Department of Immunobiology and Neuroscience, Medical Institute of Bioregulation, Kyushu University, Fukuoka 812-8582, Japan, and the [§§]Section of Hematology/Oncology, Center for Personalized Therapeutics, The University of Chicago, Chicago, Illinois 60637

Background: JMJD6 hydroxylates U2AF65, but its role in histone modification has been obscure.
Results: Our analysis of histones purified from JMJD6 knock-out mouse embryos reveals that JMJD6 hydroxylates histone lysyl residues.
Conclusion: JMJD6 mediates histone lysyl 5-hydroxylation, which is a novel histone modification.
Significance: Our study identifies a new function for Jumonji family proteins in epigenetic modification of histones.

JMJD6 is reported to hydroxylate lysyl residues of a splicing factor, U2AF65. In this study, we found that JMJD6 hydroxylates histone lysyl residues. *In vitro* experiments showed that JMJD6 has a binding affinity to histone proteins and hydroxylates multiple lysyl residues of histone H3 and H4 tails. Using JMJD6 knock-out mouse embryos, we revealed that JMJD6 hydroxylates lysyl residues of histones H2A/H2B and H3/H4 *in vivo* by amino acid composition analysis. 5-Hydroxylysine was detected at the highest level in histones purified from murine testis, which expressed JMJD6 at a significantly high level among various tissues examined, and JMJD6 overexpression increased the amount of 5-hydroxylysine in histones in human embryonic kidney 293 cells. These results indicate that histones are additional substrates of JMJD6 *in vivo*. Because 5-hydroxylation of lysyl residues inhibited *N*-acetylation and *N*-methylation by an acetyltransferase and a methyltransferase, respectively, *in vitro*, histone 5-hydroxylation may have important roles in epigenetic regulation of gene transcription or chromosomal rearrangement.

Jumonji domain containing 6 (JMJD6),[2] which possesses high binding affinity to single-stranded RNA, is reported to hydroxylate lysyl residues of an RNA splicing factor, U2AF65 (1, 2). JMJD6 contains a JmjC domain that catalyzes lysyl hydroxylation of proteins in the presence of 2-oxoglutarate, Fe(II), and ascorbate. Proteins belonging to the JmjC family are classified into 2-oxoglutarate oxygenases (3). Among the known 2-oxoglutarate oxygenases, PLOD3 (procollagen-lysine, 2-oxoglutarate 5-dioxygenase 3) mediates hydroxylation of unmodified lysyl residues, yielding 5-hydroxylysine (4). Most JmjC family members catalyze hydroxylation of *N*-methyl groups at the ϵ-amino group of lysyl residues and generate hydroxymethyl groups, which are immediately processed to formaldehyde molecules, resulting in demethylation of methylated lysyl residues (5). However, JMJD6 does not add a hydroxyl group to the *N*-methyl group but adds it to one of the backbone carbons in a lysyl side chain and generates a stable 5-hydroxylysine (1). JMJD6 knock-out mice exhibited severe anemia, growth retardation, and a delay in terminal differentiation of the kidney, intestine, liver, and lung during embryogenesis, resulting in perinatal lethality (6, 7).

In this study, we first identified JMJD6 as a novel UHRF1 (ubiquitin-like with PHD and RING finger domains 1) interacting protein. UHRF1 has important roles in transferring DNA methylation status and recognizes histone modification status (8). Therefore, we thought that JMJD6 might hydroxylate histone molecules through interaction with UHRF1. Using JMJD6 knock-out mice, we revealed that JMJD6 hydroxylates histone lysyl residues and generates 5-hydroxylysine *in vivo*. 5-Hydroxylation is a novel histone lysyl modification. Because it interfered with *N*-acetylation and *N*-methylation by an acetyltransferase and a methyltransferase, respectively, the modification may regulate transcription through these interactions with other histone modifications.

EXPERIMENTAL PROCEDURES

JMJD6 Wild-type and Knock-out Mice—Details of the JMJD6 knock-out mice were described elsewhere (6). C57BL/6 mice

* This work was supported by JSPS KAKENHI Grant 22700867 and Kyushu University interdisciplinary programs in education and projects in research development.
[1] To whom correspondence should be addressed: Div. of Epigenetics, Dept. of Molecular Genetics, Medical Institute of Bioregulation, Kyushu University, 3-1-1 Maidashi, Higashi-ku, Fukuoka-shi, Fukuoka 812-8582, Japan. Tel.: 81-92-642-6760; Fax: 81-92-642-6799; E-mail: unokim@bioreg.kyushu-u.ac.jp.
[2] The abbreviations used are: JMJD6, Jumonji domain containing 6; qRT-PCR, quantitative RT-PCR; HAT, histone acetyltransferase; E14.5, embryonic day 14.5; AdoMet, *S*-adenosyl-L-methionine.

were used as wild-type control mice. JMJD6 knock-out embryonic day 14.5 (E14.5) embryos were obtained by crossing heterozygous JMJD6 mutant mice.

Antibodies, Plasmids, and Cell Lines—The following antibodies were used: anti-JMJD6 rabbit polyclonal antibody (ab10526, Abcam), and anti-β-actin mouse monoclonal antibody (GTX26276, GeneTex). Human *JMJD6* cDNA was cloned into pGEX-6p-1 (GE Healthcare) and pcDNA5/FRT/TO (Invitrogen). Doxycycline (Dox)-inducible JMJD6 stable cells were generated using the Flp-In T-REx system (Invitrogen) according to the manufacturer's instructions. JMJD6 expression was induced by Dox (final concentration, 0.5 μg/ml; TaKaRa, Tokyo, Japan). J1 mouse ES cells were obtained from ATCC (Manassas, VA) and maintained in DMEM with 15% fetal bovine serum (FBS), nonessential amino acids, 2-mercaptoethanol, and leukemia inhibitory factor. Flp-In T-Rex 293 cells were obtained from Invitrogen and the Dox-inducible JMJD6 stable 293 cells were maintained in DMEM with 10% FBS, 10% tetracycline-free FBS, hygromycin B (100 μg/ml), and blasticidin S (15 μg/ml).

Quantitative RT-PCR—For qRT-PCR reactions, specific primers and probes for mouse JMJD6 (forward, 5′-GACCCGGCACAACTACTACG-3′; reverse, 5′-CTCTTGTGCATTGAGCAGAAC-3′) and mouse GAPDH (forward, 5′-CCATGTTTGTGATGGGTGTG-3′ and reverse, 5′-ACTGTGGTCATGAGCCCTTC-3′) were used. PCR reactions were performed using the TaKaRa Thermal Cycler Dice® Real Time System Single following the manufacturer's instructions. Amplification conditions were 30 s at 95 °C and then 40 cycles each consisting of 5 s at 95 °C and 30 s at 60 °C.

Purification of GST-JMJD6 and in Vitro Binding Assay—Recombinant GST-JMJD6 was expressed in BL21-CodonPlus DE3-RIL cells. The transformed bacteria were incubated in L-Broth media with 0.1 mM isopropyl 1-thio-β-D-galactopyranoside at 16 °C overnight. Following this, the bacteria were lysed in sonication buffer (150 mM NaCl, 20 mM Tris-HCl (pH 7.5), 2 mM EDTA, 10% glycerol, 1% Triton X, and 0.8 mg/ml lysozyme) by sonication. GST-JMJD6 was purified using glutathione-Sepharose 4FF (GE Healthcare) and eluted by glutathione. The purified proteins were incubated with biotin-labeled histone $H3_{1-21}$ peptides (12–405, Millipore, Billerica, MA) or recombinant full-length histone H4 (14–697, Millipore) in 0.1% Nonidet P-40 lysis buffer (150 mM NaCl, 0.1% Nonidet P-40, and 50 mM Tris-HCl (pH 8.0)) for 1 h at 4 °C. The biotin-labeled histone $H3_{1-21}$ peptides were pulled down with interacting proteins by streptavidin Sepharose (S951, Invitrogen). Full-length histone H4 was immunoprecipitated with anti-JMJD6 rabbit polyclonal antibody (ab10526, Abcam), which was also used for Western blotting.

In Vitro Hydroxylation Assay—To perform the enzyme assay, GST-JMJD6 was prepared as described above. Extracted GST-JMJD6 was concentrated using a 50 K column (Millipore), and its buffer was replaced with 50 mM Tris-HCl (pH 7.5) by dialysis using EasySep (TOMY, Tokyo, JAPAN). Purity of GST-JMJD6 was assessed by Coomassie Brilliant Blue staining. The enzyme assay was performed in 50 mM Tris-HCl (pH 7.5) buffer containing 500 μM α-ketoglutarate, 100 μM L-ascorbate, 100 μM $Fe(NH_4)_2SO_4$, 10 μM GST-JMJD6, and 20 μM histone peptides.

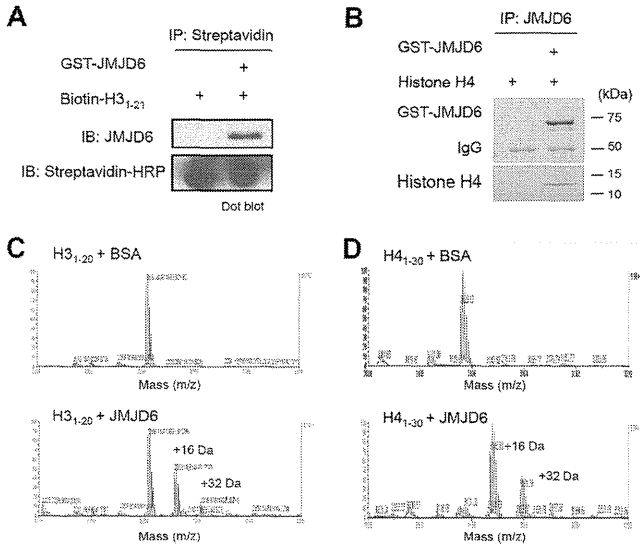

FIGURE 1. **JMJD6 interacts with and hydroxylates histone H3 and H4 *in vitro*.** *A* and *B*, *in vitro* pulldown assay. Biotin-labeled histone $H3_{1-21}$ peptides (*A*) or recombinant histone H4 (*B*) were incubated with or without GST-JMJD6, pulled down by streptavidin-Sepharose, and detected by dot blot using streptavidin-HRP (*A*) or Coomassie Brilliant Blue (*CBB*) staining (*B*). Pulled down GST-JMJD6 was detected by Western blotting using anti-JMJD6 antibody (*A*) or Coomassie Brilliant Blue staining (*B*). *C* and *D*, enzymatic activity of GST-JMJD6 was measured by MS analysis. Histone $H3_{1-20}$ (*C*) and $H4_{1-30}$ (*D*) peptides were served as substrates. BSA was used as a negative control. *IB*, immunoblot.

Protein purification and the enzyme assay were performed on the same day to avoid reduction of enzymatic activity of JMJD6.

MS Analysis—Peptides treated with JMJD6 were acidified with trifluoroacetic acid (TFA; final concentration, 0.5%) and absorbed with ZipTipC18. The captured peptides were washed with 0.1% TFA with 2% acetonitrile once and eluted with 0.5 μl of the matrix solution (4 mg/ml cyano-4-hydroxycinnamic acid, 0.1% TFA, 70% acetonitrile) onto the MALDI target plate (AB Sciex, Foster City, CA). The spotted samples were analyzed with the reflectron mode of 4800 plus MALDI-TOF-TOF mass spectrometer (AB Sciex).

Purification of Histones and Detection of 5-Hydroxylysine by Amino Acid Composition Analysis—Histones H2A/H2B and H3/H4 were separately purified from tissues or culturing cells using a histone purification kit (Active Motif, Carlsbad, CA) according to the manufacturer's instructions. The extracted histones were separated by SDS-PAGE, transferred to a membrane (Immobilon-P^{SQ}, Millipore), and stained by Coomassie Brilliant Blue. The transferred histones were used for amino acid composition analysis to detect 5-hydroxylysine.

The JMJD6-treated peptides or the purified histones were hydrolyzed in 6 N HCl vapor at 110 °C for 20 h. The acid hydrolysates of the peptides were derivatized with 6-aminoquinolyl-*N*-hydroxysuccinimidyl carbamate, and 6-aminoquinolylcarbamyl amino acid thus obtained was quantified by ion-pair chromatography using tetramethylammonium bromide on a C18-reversed phase column (L-column 2, 3.0 mm, inner diameter × 250 mm, 3 μm, CERI, Tokyo, Japan) (9). Each amino acid was separated by HPLC. The acid hydrolysates of the histones were purified on a graphitic carbon column (Hypercarb, 2.1 mm, inner diameter × 100 mm, 3 μm, Thermo Fisher Scien-

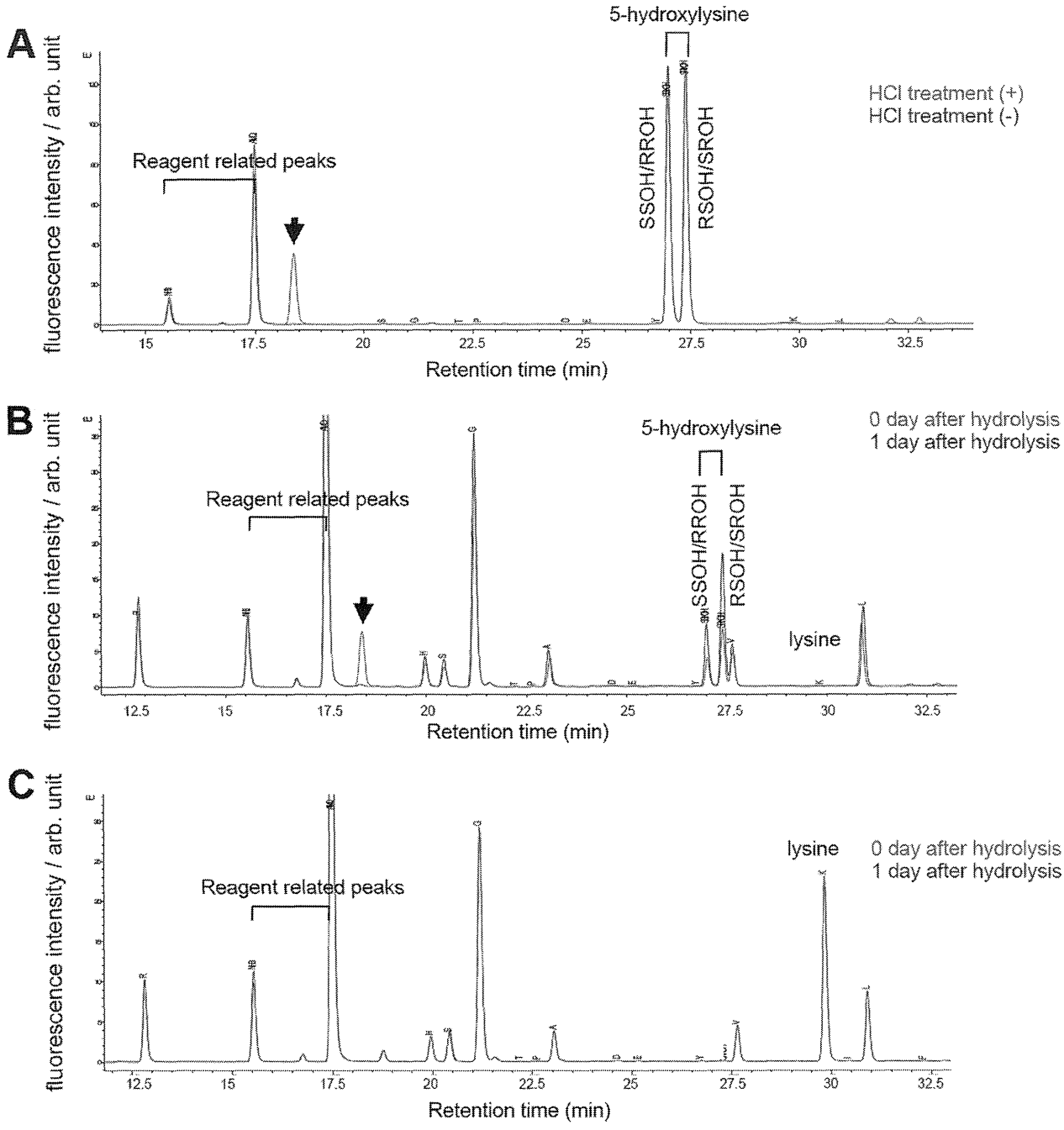

FIGURE 2. **Establishment of amino acid composition analysis for detecting 5-hydroxylysine.** *A*, analysis of simplicial synthetic SR-hydroxylysine and synthetic racemic mixture (*SS/RR/RS/SR*) of 5-hydroxylysine either treated with (*red*) or without (*blue*) HCl. *B* and *C*, analysis of $H4_{1-20}$ peptides including synthetic 5-hydroxylysine (*B*) and unmodified $H4_{1-20}$ peptides (*C*). The peptides were analyzed in the same day of hydrolysis (*red*) or next day of hydrolysis (*blue*). The *arrow* indicates a 5-hydroxylysine derived peak, which possibly corresponds to a lactone derivative, 3-amino-6-(aminomethyl)oxan-2-one. *SSOH/RROH*, 2*S*,5*S*-/2*R*,5*R*-hydroxylysine; *RSOH/SROH*, 2*R*,5*S*-/2*S*5*R*-hydroxylysine; *arb. unit*, arbitrary units.

tific, Inc., Waltham, USA), and a fraction including 5-hydroxylysine was derivatized with 6-aminoquinolylcarbamyl. The 6-aminoquinolylcarbamyl amino acids were separated on a C18-reversed phase column (Inertsustain C18HP, 3.0 mm, inner diameter × 250 mm, 3 μm, GL Sciences, Tokyo, Japan) and quantified. Synthetic racemic mixture of DL-5-hydroxylysine (catalog no. H0377, Sigma-Aldrich), and 2*S*,5*R*-hydroxylysine (catalog no. 55501, Sigma-Aldrich) were used as standards.

In Vitro Histone Acetyltransferase (HAT) Assay—The *in vitro* p300 colorimetric HAT assay was performed according to a protocol from BIOMOL (Plymouth Meeting, PA). In brief, the catalytic domain of human p300 (catalog no. SE-451, BIOMOL) and the indicated amount of control histone $H4_{1-23}$ peptides or 5-hydroxylysine containing histone $H4_{1-23}$ peptides, in which all lysines were substituted to 5-hydroxylysine (Sigma-Genosys, Hokkaido, Japan), were incubated in 50 μl of assay buffer (50 mM HEPES/NaOH (pH 7.9), 0.1 mM EDTA, 50 μg/ml BSA) in

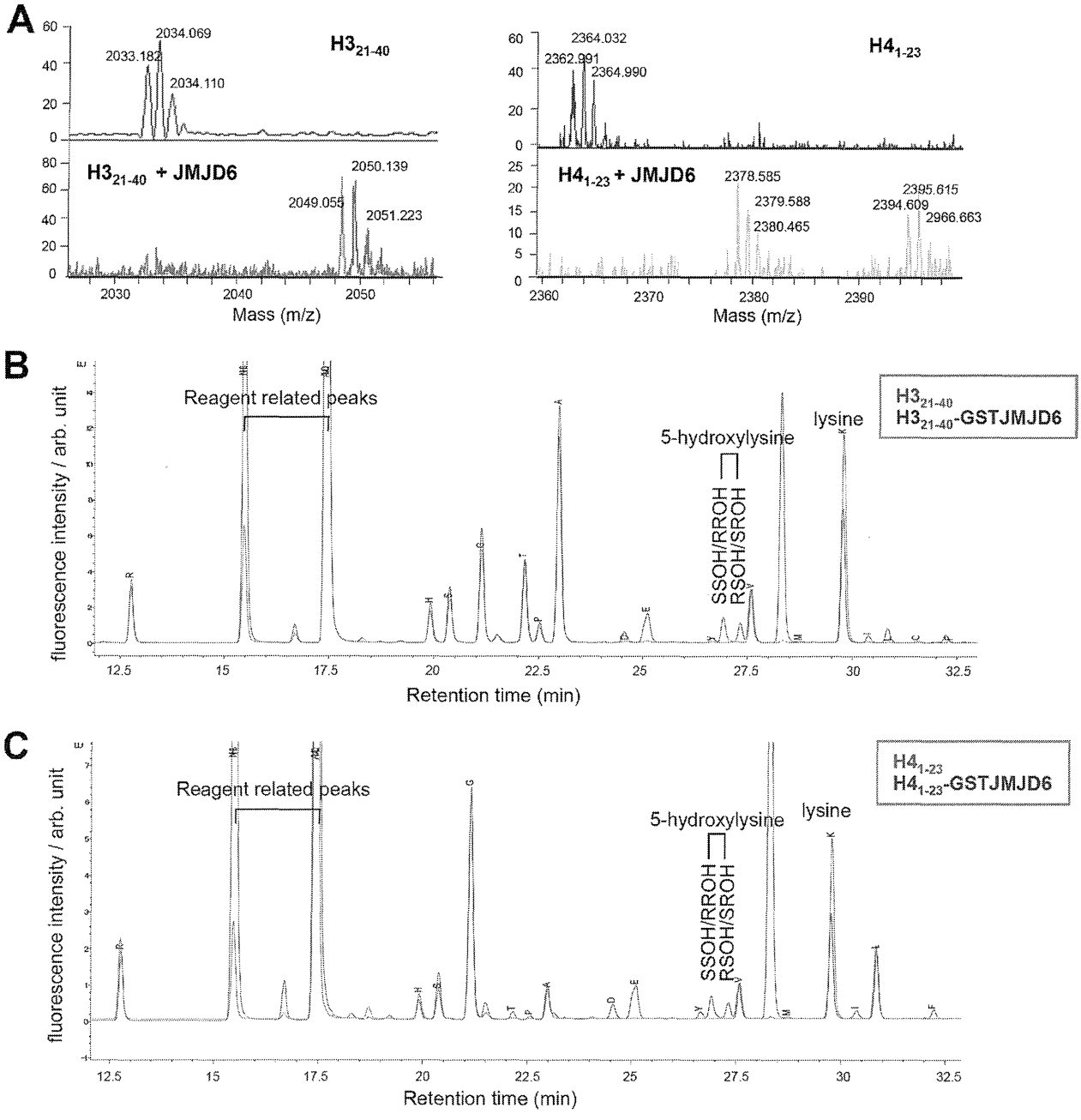

FIGURE 3. **JMJD6 hydroxylates histone H3 and H4 peptides detected by amino acid composition analysis.** *A*, hydroxylation of $H3_{21-40}$ and $H4_{1-23}$ peptides by GST-JMJD6 was confirmed by MS analysis. *B* and *C*, results of amino acid composition analysis of $H3_{21-40}$ (*B*) and $H4_{1-23}$ (*C*) peptides treated with (*blue*) or without (*red*) GST-JMJD6. *SSOH/RROH*, 2*S*,5*S*/2*R*,5*R*-hydroxylysine; *RSOH/SROH*, 2*R*,5*S*-/2*S*,5*R*-hydroxylysine; *arb. unit*, arbitrary units.

the presence of acetyl-coenzyme A (CoA, Sigma-Aldrich) at 37 °C. The reaction was stopped by adding 100 μl of quenching buffer (3.2 M guanidinium HCl, 100 mM Na_2HPO_4/NaH_2PO_4 (pH6.8)) at the indicated times. Following this, 50 μl of 2 mM 5,5′-dithiobis-2-nitrobenzoic acid (Sigma-Aldrich) in 100 mM Na_2HPO_4/NaH_2PO_4 (pH 6.8) was added, and absorbance at 405 nm was read by a spectrophotometer (ARVO MX/Light 1420 Multilabel/Luminescence Counter, PerkinElmer Life Sciences). The transfer of an acetyl group from an acetyl-CoA to the ϵ-amino group of lysine residues was quantified by measurement of the thiol group of CoA. A standard curve was generated using β2-mercaptoethanol.

In Vitro Histone Methyltransferase Assay—The *in vitro* histone methyltransferase assay was performed as described previously (10), except for slight modifications. In brief, a fixed amount of purified baculovirus-produced recombinant SMYD3 (1 μM) was incubated with indicated histone peptides, which were also used for the *in vitro* HAT assay, and 1 μCi of *S*-adenosyl-L-methionine (AdoMet; GE Healthcare) as the methyl donor in a mixture of 60 μl of methylase activity buffer (50 mM Tris-HCl (pH 8.5), 100 mM NaCl, 10 mM dithiothreitol) at 30 °C. The incorporated ^3H-labeled methyl groups in the substrates were measured by a scintillation counter after filter binding (units, cpm). The concentration

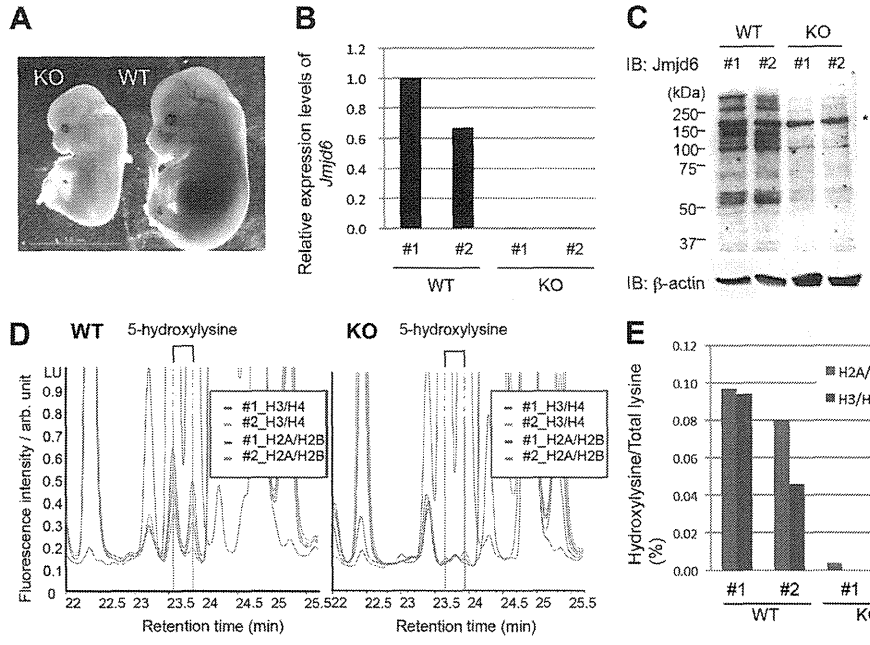

FIGURE 4. **JMJD6 hydroxylates histones H2A/H2B and H3/H4 in mouse embryos.** *A*, a representative image of JMJD6 knock-out and wild-type E14.5 embryos. *B*, *JMJD6* knock-out was confirmed by qRT-PCR. GAPDH was used as an internal control. *C*, JMJD6 knock-out was confirmed by Western blotting. The *asterisk* indicates a nonspecific band. β-Actin was used as a loading control. *D*, result of amino acid composition analysis of histones derived from two Jmjd6 wild-type (*left*) and knock-out (*right*) E14.5 embryos. *E*, % of 5-hydroxylysine in total lysine of histones H2A/H2B (*blue*) and H3/H4 (*red*) was calculated from the HPLC data (*D*). *IB*, immunoblot; *arb. unit*, arbitrary units.

(nM) of the methylated substrate was calculated based on the basis of radioactivity.

RESULTS

JMJD6 Effectively Hydroxylates Histone Lysyl Residues in Vitro—During screening of UHRF1-interacting proteins, we identified JMJD6 as a novel binding partner of UHRF1 (data not shown). Because UHRF1 recognizes hemimethylated DNA and histone modifications, we assumed that JMJD6 might be recruited by UHRF1 to nucleosomes and modify histone lysyl residues. *In vitro* experiments showed that recombinant GST-JMJD6 possessed the ability to bind to histone $H3_{1-20}$ tail and histone H4 (Fig. 1, *A* and *B*) and hydroxylate multiple lysyl residues in the N-terminal tails of histone $H3_{1-20}$ and $H4_{1-30}$, which was detected as of 16, 32, or 48 Da shifts by MS analysis (Fig. 1, *C* and *D*); subsequent MS/MS analysis revealed that JMJD6 mediates monohydroxylation of lysyl residues. As indicated by Webby *et al.* (1), JMJD6 preferentially hydroxylated lysyl residues in the basic peptides, and no apparent sequence preference was observed *in vitro* (data not shown).

Next, we established a sensitive hydroxylysine detection method based on amino acid composition analysis as an alternative to the MS-based method. For amino acid composition analysis, we briefly hydrolyzed peptides or proteins with HCl and separated each amino acid residue by reversed phase HPLC to detect 5-hydroxylysine. To evaluate this method, we first performed reversed phase HPLC using simplicial synthetic 2*S*,5*R*-hydroxylysine and synthetic racemic mixture of 5-hydroxylysine composed of 2*S*,5*S* (*SS*)-, 2*R*,5*R* (*RR*)-, 2*R*,5*S* (*RS*)-, and 2*S*,5*R* (*SR*)-stereoisomers (Fig. 2*A*). We detected two peaks corresponding to *SS*/*RR*- and *RS*/*SR*-hydroxylysine by analyzing these synthetic 5-hydroxylysines without HCl treatment (Fig. 2*A*). After HCl treatment of these synthetic 5-hydroxylysines, another peak was appeared (Fig. 2*A*, *arrow*). This peak possibly corresponds to a lactone derivative, 3-amino-6-(aminomethyl)oxan-2-one, generated by dehydration condensation between C5 hydroxyl group and carboxyl group, which is described in a previous report (11). Next, we evaluated the method using unmodified $H4_{1-23}$ peptides and 5-hydroxylysine containing $H4_{1-23}$ peptides in which all the lysines at positions 5, 8, 12, and 20 were substituted with 5-hydroxylysines. After hydrolysis of these peptides, we detected two peaks corresponding to *SS*/*RR*- and *RS*/*SR*-hydroxylysine only in the 5-hydroxylysine containing peptides but not in the unmodified peptides (Fig. 2, *B* and *C*). We also detected the peak of the possible lactone derivative in the 5-hydroxylysine containing peptides by reversed phase HPLC performed in the same day of hydrolysis, but the peak disappeared in the next day of hydrolysis, indicating that the derivative is unstable. Because quantification of the derivative is technically difficult, we only quantified *SS*/*RR*- and *RS*/*SR*-hydroxylysine.

Using this method, we analyzed $H3_{21-40}$ and $H4_{1-23}$ peptides treated with or without recombinant GST-JMJD6. First, we confirmed hydroxylation of the peptides by GST-JMJD6 by MS analysis (Fig. 3*A*). Then, the peptides were separated from the enzyme reaction mixture, by reversed phase HPLC. The separated peptides were treated with HCl, and each amino acid residue was separated by reversed phase HPLC (Fig. 3, *B* and *C*). Comparison of the chromatograph between amino acids derived from the JMJD6-treated and -untreated peptides identified two additional peaks in the peptides treated with JMJD6, which are matched with the standard synthetic 5-hydroxylysine (Fig. 3, *B* and *C*).

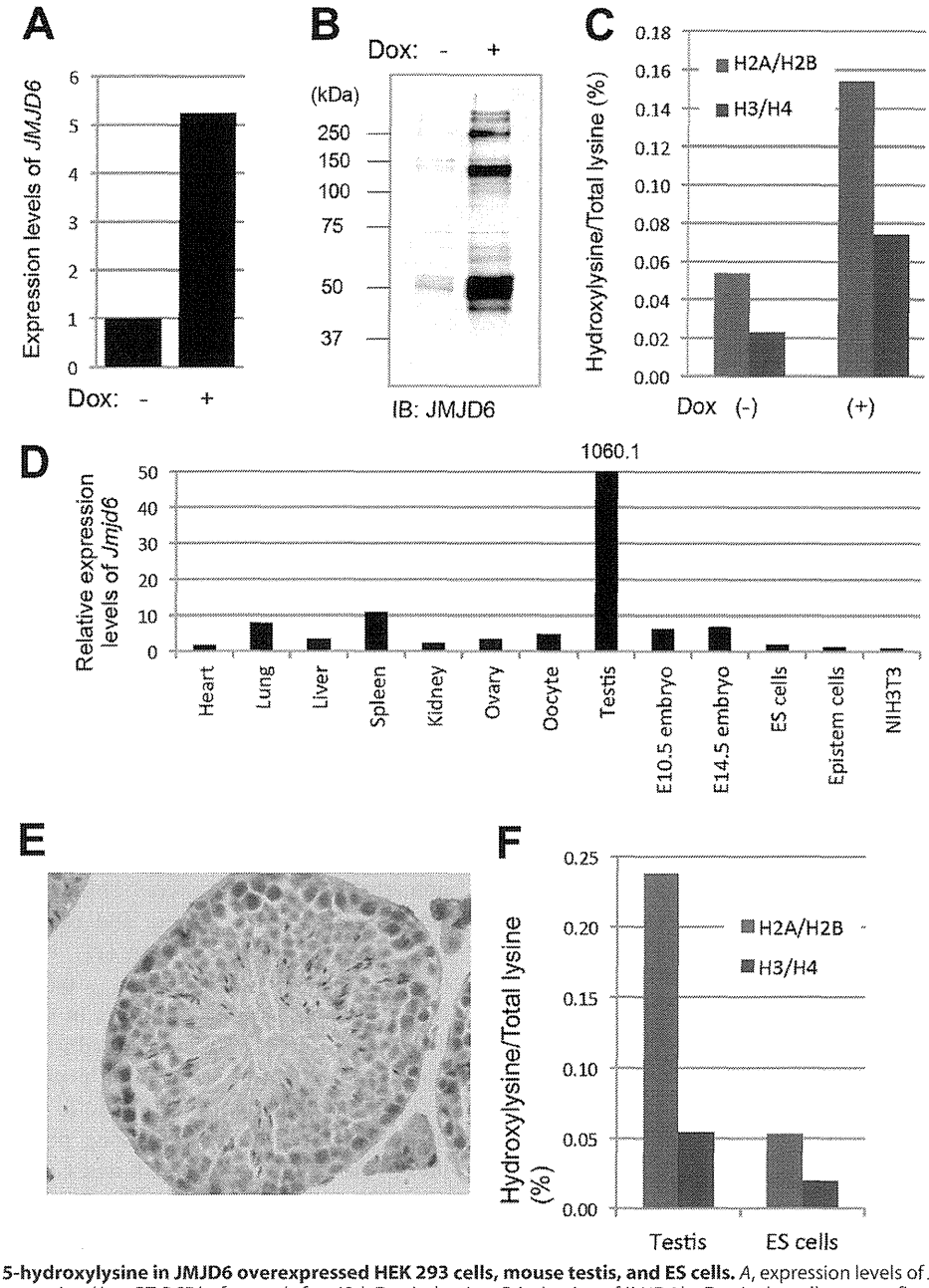

FIGURE 5. **Amount of 5-hydroxylysine in JMJD6 overexpressed HEK 293 cells, mouse testis, and ES cells.** *A*, expression levels of *JMJD6* in Dox-inducible JMJD6 stable cells were examined by qRT-PCR before and after 48-h Dox induction. *B*, induction of JMJD6 by Dox in the cells was confirmed by Western blotting. *C*, amino acid composition analysis of histones derived from Dox-inducible JMJD6 stable cell lines. The *blue* and *red bars* indicate % of 5-hydroxylysine in the total lysine of histone H2A/H2B and in the H3/H4, respectively. *D*, relative expression levels of *Jmjd6* in various mouse tissues and cells were examined by qRT-PCR. *E*, expression of Jmjd6 in a 6-month-old mouse testis was examined by immunohistochemistry. *F*, amino acid composition analysis of histones derived from 6-month-old mouse testis and J1 ES cells. The *blue* and *red bars* indicate % of 5-hydroxylysine in the total lysine of histone H2A/H2B and in the H3/H4, respectively.

JMJD6 Hydroxylates Histone Lysyl Residues in Vivo—To investigate histone lysyl hydroxylation *in vivo*, we performed the amino acid composition analysis for analyzing a mixture of histone H2A/H2B and a mixture of histone H3/H4 proteins isolated from two JMJD6 wild-type and two JMJD6 knock-out whole embryos at E14.5 (Fig. 4*A*). JMJD6 knock-out was confirmed by qRT-PCR and Western blotting (Fig. 4, *B* and *C*). The results showed that 0.097 and 0.080% of total lysyl residues in histone H2A/H2B and 0.094 and 0.046% of those in histone H3/H4 were 5-hydroxylated in each of the two JMJD6 wild-type mice (Fig. 4, *D* and *E*), whereas 0.004 and 0.011% of total lysyl residues in histone H2A/H2B and 0.000 and 0.000% of those in histone H3/H4 were 5-hydroxylated in each of the two JMJD6 knock-out mice (Fig. 4, *D* and *E*), indicating that JMJD6 hydroxylates histone lysyl residues *in vivo*.

We also generated Dox-inducible JMJD6 stable HEK293 cells. JMJD6 induction by Dox was confirmed by qRT-PCR and Western blotting (Fig. 5, *A* and *B*) and increased 5-hydroxylation levels of histone lysyl residues (Fig. 5*C*). In addition, we purified histones from a 6-month-old JMJD6 wild-type mouse

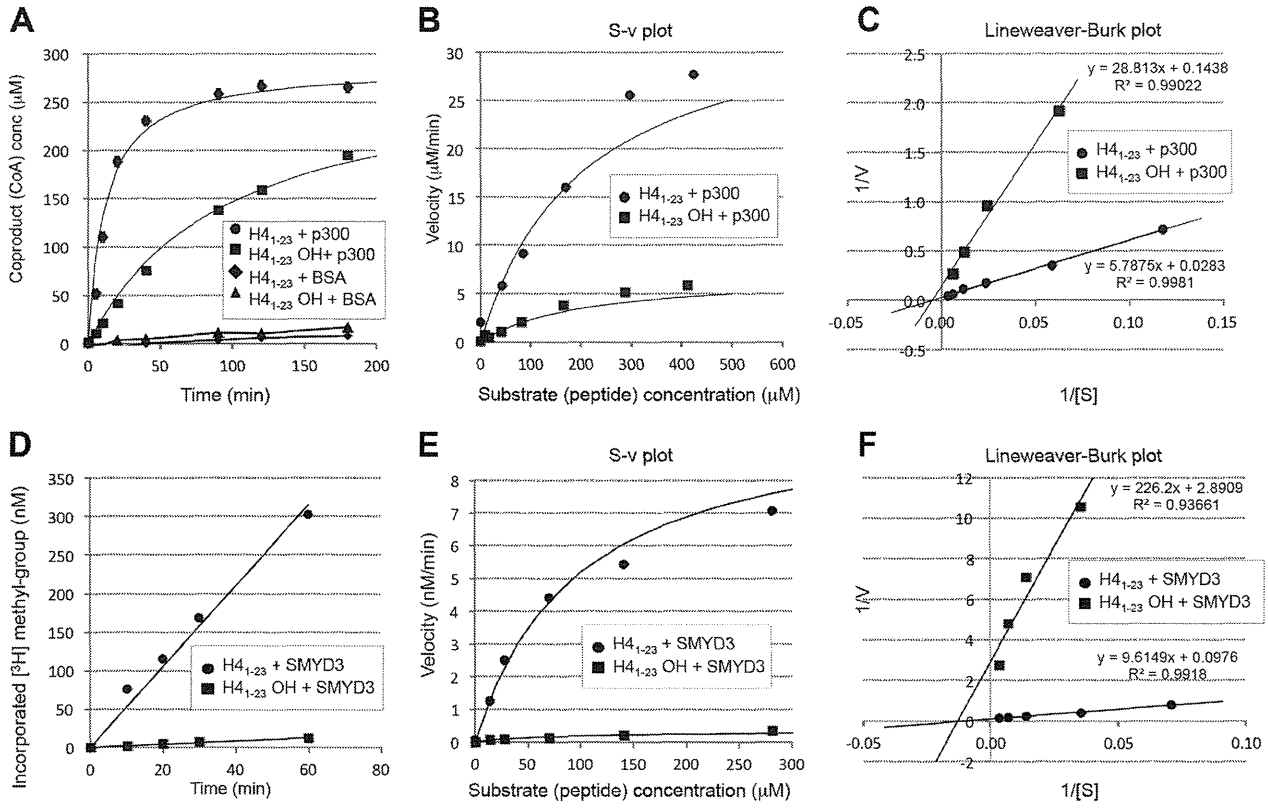

FIGURE 6. **5-Hydroxylation of lysyl residue impairs *N*-acetylation and *N*-methylation *in vitro*.** *A–C*, the *in vitro* colorimetric HAT assay was performed using a fixed amount of p300 (0.44 μM) and control H4$_{1-23}$ peptides (●) or 5-hydroxylysine-containing peptides (H4$_{1-23}$ OH, ■). BSA was used as a negative control (◆, ▲). After the reactions, absorbance (405 nm) of the coproduct (CoA) was measured. *A*, reactions were terminated at the indicated time points, and the concentration of CoA was calculated on the basis of a standard curve that was generated from β2-mercaptoethanol. *B* and *E*, substrate concentration-velocity (s-v) plot. *C* and *F*, Lineweaver-Burk plot. The *vertical axis* is 1/velocity [v], and the *horizontal axis* is 1/substrate concentration [S]. *D–F*, the *in vitro* histone methyltransferase assay was performed using a fixed amount of SMYD3 (1 μM) and control H4$_{1-23}$ peptides (●) or 5-hydroxylysine-containing peptides (H4$_{1-23}$OH, ■). AdoMet was used as a methyl donor. After the reactions, radioactivity (cpm) of the ^{3}H-methylated substrates was measured. The concentration of incorporated ^{3}H-methyl groups (nM) was calculated on the basis of radioactivity (1 cpm was 0.02563 nM in the reaction). *D*, reactions were performed with fixed amounts of the peptides (141 μM) and terminated at the indicated time points.

testis, which expressed JMJD6 at the highest level among various tissues and cells (Fig. 5, *D* and *E*). In the testis, 0.238 and 0.054% of total lysyl residues in histone H2A/H2B and H3/H4, respectively, were 5-hydroxylated (Fig. 5*F*). In the mouse J1 ES cells, 0.053 and 0.020% of total lysyl residues in histone H2A/H2B and H3/H4, respectively, were 5-hydroxylated (Fig. 5*F*).

5-Hydroxylation Prevents N-Acetylation and N-Methylation of Histone Lysyl Residues in Vitro—Because lysyl residues in histone tails are often subjected to *N*-acetylation and *N*-methylation, we examined whether 5-hydroxylation of lysyl residues affects modifications at the ϵ-amino groups. First, we examined the effect of lysyl 5-hydroxylation on histone H4 *N*-acetylation by p300, which catalyzes *N*-acetylation of the ϵ-amino group of lysyl residues, including histone H4K5 and H4K8, through its HAT domain (12). Kinetic analysis using the unmodified and the 5-hydroxylysine containing H4$_{1-23}$ peptides in which all the lysines were substituted with 5-hydroxylysines as substrates revealed that 5-hydroxylation largely interfered with the HAT activity of p300 *in vitro* (Fig. 6, *A–C*). Lineweaver-Burk plot analysis was performed to calculate the maximum velocity (V_{max}) and Michaelis constant (K_m) values (Table 1; Fig. 6*C*, $R^2 = 0.9981$ and 0.9902). V_{max} of the reactions in which p300 acetylated the 5-hydroxylysine-containing peptides (H4$_{1-23}$OH) was 5-fold less than that of the control peptides (6.95 ± 0.45 and 35.34 ± 1.65 μM/min, respectively), whereas K_m of the two reactions was quite similar (204.51 ± 10.12 and 200.37 ± 14.32 μM, respectively), indicating that 5-hydroxylation does not inhibit binding of lysyl residues to p300 but reduces the catalytic efficiency.

TABLE 1

Effect of 5-hydroxylation on *N*-acetylation of ϵ-amino group of lysyl residues

Lineweaver-Burk plots were used for estimation of the kinetic constants, V_{max}, and K_m. R^2 is the determination coefficient (see Fig. 6*C*).

	V_{max}	K_m
	μM/min	μM
H4$_{1-23}$ + p300	35.34 ± 1.65 (R^2 = 0.9981)	204.51 ± 10.12
H4$_{1-23}$ OH + p300	6.95 ± 0.45 (R^2 = 0.9902)	200.37 ± 14.32

TABLE 2

Effect of 5-hydroxylation on *N*-methylation of ϵ-amino group of lysyl residues

Lineweaver-Burk plots were used for estimation of the kinetic constants, V_{max}, and K_m. R^2 is the determination coefficient (see Fig. 6*F*).

	V_{max}	K_m
	nM/min	
H4$_{1-23}$ + SMYD3	10.90 ± 0.92 (R^2 = 0.9918)	80.63 ± 16.26 μM
H4$_{1-23}$ OH + SMYD3	0.48 ± 0.26 (R^2 = 0.9366)	75.26 ± 9.60 μM

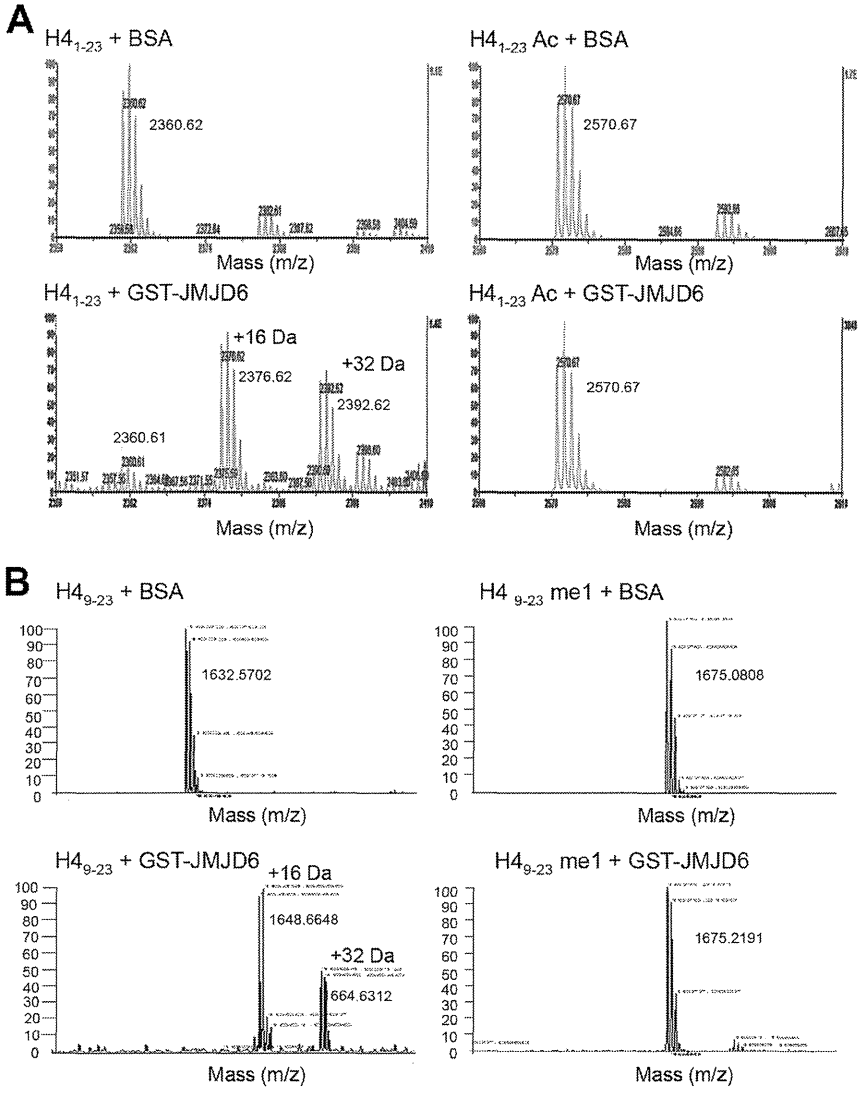

FIGURE 7. ***N*-Acetylation and *N*-methylation of lysyl residues impairs 5-hydroxylation by JMJD6 *in vitro*.** *A*, the *in vitro* hydroxylation assay was performed using GST-JMJD6 (10 μM) and 85 μM of control $H4_{1-23}$ peptides or *N*-acetyl-lysine-containing peptides. *B*, the *in vitro* hydroxylation assay was performed using GST-JMJD6 (10 μM) and 85 μM control $H4_{1-23}$ peptides or *N*-monomethyl-lysine-containing peptides. BSA was used as a negative control. 5-Hydroxylation by JMJD6 was detected by MS analysis.

We also examined the effect of lysyl 5-hydroxylation on the histone methyltransferase activity of SMYD3, which catalyzes lysyl *N*-methylation of histone H3 (13) and also H4 (data not shown) through its SET (su(var) 3–9 enhancer-of-zeste trithorax) domain by the histone methyltransferase assay. The results showed that 5-hydroxylation at lysyl residues almost completely inhibited *N*-methylation catalyzed by SMYD3 (Table 2 and Fig. 6, *D–F*); V_{max} values of the reactions with the control peptides ($H4_{1-23}$) and the 5-hydroxylysine-containing peptides ($H4_{1-23}$OH) as substrates were 10.90 ± 0.92 and 0.48 ± 0.26 nM/min, respectively. Similar to the HAT assay, K_m values of the two reactions were ~80.63 ± 16.26 and 75.26 ± 9.60 μM, respectively.

Subsequently, we performed reciprocal experiments using $H4_{1-23}$ or $H4_{9-23}$ peptides, in which all the lysines are either unmodified, *N*-acetylated, or *N*-monomethylated. JMJD6 effectively hydroxylated the control peptides (Fig. 7, *A* and *B*, *left panels*); however, *N*-acetylation and *N*-monomethylation at the ϵ-amino group of the lysines completely blocked 5-hydroxylation by JMJD6 (Fig. 7, *A* and *B*, *right panels*).

DISCUSSION

We found a novel histone modification, 5-hydroxylation, by JMJD6. JMJD6 reportedly hydroxylates a splicing factor, U2AF65 (1). That study and another report (1, 14) stated that evidence of histone lysyl hydroxylation was not found by MS-based analysis *in vivo*. In the present study, we developed an alternative method, amino acid composition analysis, to detect 5-hydroxylation of histone lysyl residues. As reported previously, we have not detected clear evidence of 5-hydroxylation of histone lysyl residues by MS-based analysis. We think that there are several causes for this. 1) The amount of 5-hydroxylysine is too small to detect by MS-based analysis. 2) Artificial methionine oxidation during preparation of samples for MS analysis

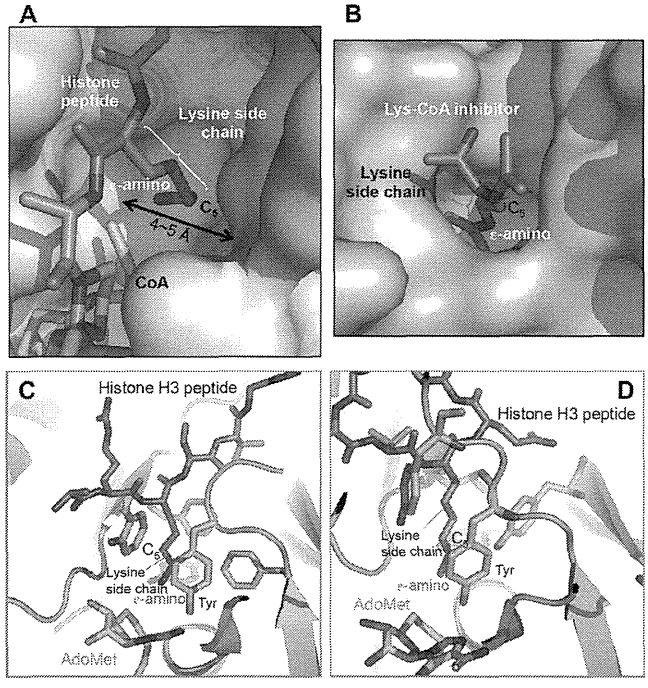

FIGURE 8. **Structure around the active site of HAT domains and SET domains, a lysine side chain, and an *S*-adenosyl methionine (*AdoMet*).** *A*, spatial localization among the HAT domain of GCN5 (*gray*), a lysine side chain (*magenta*), and CoA (*cyan*) (Protein Data Bank code 1QSN). The 5-hydroxyl group may locate close to acetyl-CoA, indicating that this may work as a steric barrier and prevent effective *N*-acetylation by the catalytic domain. *B*, structure of the HAT domain of p300 (*gray*) in complex with inhibitor, Lys-CoA (*magenta*) (Protein Data Bank code 3BIY). The 5-hydroxyl group may restrict the conformation of lysine side chain in the catalytic pocket of p300. The figures were prepared by using program PyMOL. *C*, spatial localization among the SET domain of *N. crassa* Dim-5 (*green*), a histone H3 peptide (*magenta*), and AdoMet (*cyan*) (Protein Data Bank code 1PEG). *D*, spatial association among the SET domain of human SETD7/9 (*green*), a histone H3 peptide containing monomethylated Lys-4 (*magenta*), and AdoMet (*cyan*) (Protein Data Bank code 1O9S). A side chain of a lysine residue locates in tightly hydrophobic pocket of the SET domains (*C* and *D*). Hydroxylation at position C_5 of the chain may prevent a lysine side chain to locate in the pocket, causing inhibition of *N*-methylation by SET domains.

makes detection of 5-hydroxylysine difficult. 3) 5-Hydroxylysine could be an intermediate form as it is in collagen, and a further unknown modification(s) such as glycosylation could be added; the final product of collagen is glucosylgalactosyl hydroxylysine (4). The collagen hydroxylase, PLOD3, possesses galactosyltransferase and glucosyltransferase activities. Unlike PLOD3, JMJD6 does not appear to possess any other enzymatic activities by domain search; therefore, it is difficult to assume possible further modification(s) by its protein structure. We may have been able to detect 5-hydroxylation in histone lysyl residues by amino acid composition analysis but not by the MS-based analysis because many modifications such as glycosylation or galactosylation could be removed during the hydrolysis process of amino acid composition analysis. By this analysis, we detected both *SS*/*RR*- and *SR*/*RS*-hydroxylysine in JMJD6-treated histone peptides and also in JMJD6 wild-type E14.5 embryos, ES cells, and the Dox-inducible JMJD6 stable HEK293 cells. Because the relationship between *RR* and *RS* and also between *SS* and *RS* is a diastereomer, we were able to distinguish them. However, because a relationship between *SS* and *RR*, and also between *RS* and *SR* is an enantiomer, we were not able to separate them by this method. Despite this, these two peaks are most likely *SS*- and *RS*-hydroxylysine because JMJD6 is reported to generate *SS*-hydroxylysine (11). The *RS*-hydroxylysine could be generated from *SS*-hydroxylysine through the lactone derivative, 3-amino-6-(aminomethyl)oxan-2-one, which is unstable and difficult to be quantified. Because of this difficulty, we only quantified *SS*/*RR*- and *RS*/*SR*-hydroxylysine in this report. Therefore, actual quantity of 5-hydroxylysine in the samples examined here could be a little higher.

Because we detected 5-hydroxylysines in the UHRF1 KO ES cells (data not shown), UHRF1 is not required for 5-hydroxylation of histone lysyl residues by JMJD6. Therefore, biological significance of the interaction between UHRF1 and JMJD6 remains unclear. Further analysis is also required to determine the biological significance of 5-hydroxylation of histone lysyl residues. *In vitro* experiments suggest that 5-hydroxylation can inhibit *N*-acetylation and *N*-methylation by p300 and SMYD3. The active site structure of the p300 and general control of amino acid synthesis 5 (GCN5) HAT domains showed that the side chain of the 5-hydroxylysine can invade the catalytic pocket; however, the 5-hydroxyl group may disturb active form formation of the substrate (Fig. 8, *A* and *B*). The catalytic site of SET domains of *Neurospora crassa* Dim-5 and human SETD7, which are structurally similar to SMYD3 (15), suggested that the side chain of 5-hydroxylysine can invade the catalytic pocket; however, the 5-hydroxyl group may disturb an active form formation of the substrate (16, 17) similar to that in HAT domains (Fig. 8, *C* and *D*). Therefore, 5-hydroxylation could be important in the context of the histone code. It is known that histones H2A and H2B move more dynamically between the nucleosome and nucleoplasm. 5-Hydroxylation of these histones may have some effects for the movement because the modification was detected more in histones H2A/H2B than in histones H3/H4. The expression pattern of JMJD6 is also interesting. JMJD6 may play important role(s) in the testis, such as a role in histone-protamine exchange. We believe that our present finding provides a novel insight into epigenetic regulations of gene transcription and/or chromosomal rearrangement.

Acknowledgments—We thank Dr. Haruhiko Koseki and Dr. Jafar Sharif for providing us UHRF1 KO ES cells; Professor Shoji Tajima, Dr. Isao Suetake, Dr. Yoichi Shinkai, Dr. Kenji Ichiyanagi, Dr. Fumiyuki Sanematsu, and Dr. Hyun-Soo Cho for useful advice; and Yuichi Mishima and Dr. Atsuhiko Toyama for technical assistance.

REFERENCES

1. Webby, C. J., Wolf, A., Gromak, N., Dreger, M., Kramer, H., Kessler, B., Nielsen, M. L., Schmitz, C., Butler, D. S., Yates, J. R., 3rd, Delahunty, C. M., Hahn, P., Lengeling, A., Mann, M., Proudfoot, N. J., Schofield, C. J., and Böttger, A. (2009) Jmjd6 catalyses lysyl-hydroxylation of U2AF65, a protein associated with RNA splicing. *Science* **325**, 90–93
2. Hong, X., Zang, J., White, J., Wang, C., Pan, C. H., Zhao, R., Murphy, R. C., Dai, S., Henson, P., Kappler, J. W., Hagman, J., and Zhang, G. (2010) Interaction of JMJD6 with single-stranded RNA. *Proc. Natl. Acad. Sci. U.S.A.* **107**, 14568–14572
3. Loenarz, C., and Schofield, C. J. (2008) Expanding chemical biology of 2-oxoglutarate oxygenases. *Nat. Chem. Biol.* **4**, 152–156
4. Myllylä, R., Wang, C., Heikkinen, J., Juffer, A., Lampela, O., Risteli, M., Ruotsalainen, H., Salo, A., and Sipilä, L. (2007) Expanding the lysyl hydrox-

ylase toolbox: new insights into the localization and activities of lysyl hydroxylase 3 (LH3). *J. Cell. Physiol.* **212,** 323–329
5. Shi, Y., and Whetstine, J. R. (2007) Dynamic regulation of histone lysine methylation by demethylases. *Mol. Cell* **25,** 1–14
6. Kunisaki, Y., Masuko, S., Noda, M., Inayoshi, A., Sanui, T., Harada, M., Sasazuki, T., and Fukui, Y. (2004) Defective fetal liver erythropoiesis and T lymphopoiesis in mice lacking the phosphatidylserine receptor. *Blood* **103,** 3362–3364
7. Böse, J., Gruber, A. D., Helming, L., Schiebe, S., Wegener, I., Hafner, M., Beales, M., Köntgen, F., and Lengeling, A. (2004) The phosphatidylserine receptor has essential functions during embryogenesis but not in apoptotic cell removal. *J. Biol.* **3,** 15
8. Unoki, M., Brunet, J., and Mousli, M. (2009) Drug discovery targeting epigenetic codes: the great potential of UHRF1, which links DNA methylation and histone modifications, as a drug target in cancers and toxoplasmosis. *Biochem. Pharmacol.* **78,** 1279–1288
9. Masuda, A., and Dohmae, N. (2010) Automated Protein Hydrolysis Delivering Sample to a Solid Acid Catalyst for Amino Acid Analysis. *Anal. Chem.* **82,** 8939–8945
10. Strahl, B. D., Ohba, R., Cook, R. G., and Allis, C. D. (1999) Methylation of histone H3 at lysine 4 is highly conserved and correlates with transcriptionally active nuclei in *Tetrahymena*. *Proc. Natl. Acad. Sci. U.S.A.* **96,** 14967–14972
11. Mantri, M., Loik, N. D., Hamed, R. B., Claridge, T. D., McCullagh, J. S., and Schofield, C. J. (2011) The 2-oxoglutarate-dependent oxygenase JMJD6 catalyses oxidation of lysine residues to give 5S-hydroxylysine residues. *Chembiochem.* **12,** 531–534
12. Schiltz, R. L., Mizzen, C. A., Vassilev, A., Cook, R. G., Allis, C. D., and Nakatani, Y. (1999) Overlapping but distinct patterns of histone acetylation by the human coactivators p300 and PCAF within nucleosomal substrates. *J. Biol. Chem.* **274,** 1189–1192
13. Hamamoto, R., Furukawa, Y., Morita, M., Iimura, Y., Silva, F. P., Li, M., Yagyu, R., and Nakamura, Y. (2004) SMYD3 encodes a histone methyltransferase involved in the proliferation of cancer cells. *Nat. Cell Biol.* **6,** 731–740
14. Han, G., Li, J., Wang, Y., Li, X., Mao, H., Liu, Y., and Chen, C. D. (2012) The hydroxylation activity of Jmjd6 is required for its homo-oligomerization. *J. Cell. Biochem.* **113,** 1663–1670
15. Dillon, S. C., Zhang, X., Trievel, R. C., and Cheng, X. (2005) The SET-domain protein superfamily: protein lysine methyltransferases. *Genome Biol.* **6,** 227
16. Zhang, X., Tamaru, H., Khan, S. I., Horton, J. R., Keefe, L. J., Selker, E. U., and Cheng, X. (2002) Structure of the Neurospora SET domain protein DIM-5, a histone H3 lysine methyltransferase. *Cell* **111,** 117–127
17. Subramanian, K., Jia, D., Kapoor-Vazirani, P., Powell, D. R., Collins, R. E., Sharma, D., Peng, J., Cheng, X., and Vertino, P. M. (2008) Regulation of estrogen receptor α by the SET7 lysine methyltransferase. *Mol. Cell* **30,** 336–347

Journal of proteome research

Article

pubs.acs.org/jpr

Plasma Low-Molecular-Weight Proteome Profiling Identified Neuropeptide-Y as a Prostate Cancer Biomarker Polypeptide

Koji Ueda,*[,†] Ayako Tatsuguchi,[†] Naomi Saichi,[†] Atsuhiko Toyama,[‡] Kenji Tamura,[§] Mutsuo Furihata,[∥] Ryo Takata,[⊥] Shusuke Akamatsu,[#] Masahiro Igarashi,[▽] Masato Nakayama,[○] Taka-Aki Sato,[‡] Osamu Ogawa,[#] Tomoaki Fujioka,[⊥] Taro Shuin,[§] Yusuke Nakamura,[◆] and Hidewaki Nakagawa[†]

[†]Laboratory for Biomarker Development, Center for Genomic Medicine, RIKEN, General Research Building 6F, Institute of Medical Science, 4-6-1, Shirokanedai, Minato-ku, Tokyo 108-8639, Japan

[‡]Life Science Research Center, Shimadzu Corporation, 1-3, Nishikicho, Kanda, Chiyoda-ku, Tokyo 101-8448, Japan

[§]Department of Urology, Kochi Medical School Hospital, Oko-cho Kohasu, Nankoku-shi, Kochi 783-8505, Japan

[∥]Department of Pathology, Kochi Medical School, Oko-cho Kohasu, Nankoku-shi, Kochi 783-8505, Japan

[⊥]Department of Urology, Iwate Medical University, 19-1 Uchimaru, Morioka, Iwate Prefecture 020-0023, Japan

[#]Department of Urology, Graduate School of Medicine, Kyoto University, Yoshida-Konoe-cho, Sakyo-ku, Kyoto 606-8501, Japan

[▽]Endoscopy Division, Gastrointestinal Center, Cancer Institute Hospital, 3-8-31, Ariake, Koto, Tokyo 135-8550, Japan

[○]Toppan Printing Co., Ltd., 1-5-1, Taito, Taito-ku, Tokyo 110-8560, Japan

[◆]Section of Hematology/Oncology, Department of Medicine Faculty, The University of Chicago, 5841 South Maryland Avenue, Chicago, Illinois, United States

S *Supporting Information*

ABSTRACT: In prostate cancer diagnosis, PSA test has greatly contributed to the early detection of prostate cancer; however, expanding overdiagnosis and unnecessary biopsies have emerged as serious issues. To explore plasma biomarkers complementing the specificity of PSA test, we developed a unique proteomic technology QUEST-MS (Quick Enrichment of Small Targets for Mass Spectrometry). The QUEST-MS method based on 96-well formatted sequential reversed-phase chromatography allowing efficient enrichment of <20 kDa proteins quickly and reproducibly. Plasma from 24 healthy controls, 19 benign prostate hypertrophy patients, and 73 prostate cancer patients were purified with QUEST-MS and analyzed by LC/MS/MS. Among 153 057 nonredundant peptides, 189 peptides showed prostate cancer specific detection pattern, which included a neurotransmitter polypeptide neuropeptide-Y (NPY). We further validated the screening results by targeted multiple reaction monitoring technology using independent sample set (n = 110). The ROC curve analysis revealed that logistic regression-based combination of NPY, and PSA showed 81.5% sensitivity and 82.2% specificity for prostate cancer diagnosis. Thus QUEST-MS technology allowed comprehensive and high-throughput profiling of plasma polypeptides and had potential to effectively uncover very low abundant tumor-derived small molecules, such as neurotransmitters, peptide hormones, or cytokines.

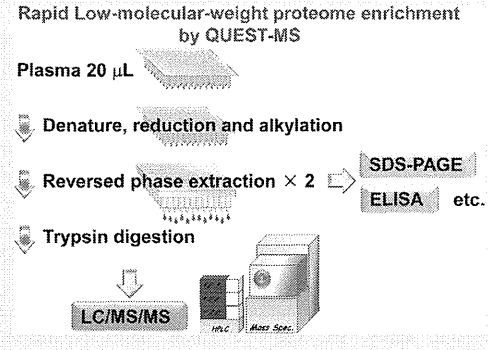

KEYWORDS: *low molecular weight, Biomarker, prostate cancer, plasma, PSA, mass spectrometry, label-free quantification*

INTRODUCTION

Prostate-specific antigen (PSA), also known as kallikrein-3, was discovered in 1969[1] and had been recognized as the best diagnostic tool for prostate cancer since the Food and Drug Administration (FDA) approved the PSA test in 1994.[2] Indeed, at least 30 million men over 50 years old undergo PSA test in the United States in a year. However, in October 2011, the U.S. Preventive Services Task Force (USPSTF) published statistical evidence about clinical outcomes of prostate cancer and urged not to continue PSA test against healthy males anymore.[3] This decision was simply based on the concept that the benefit of PSA test to overall survival rate of prostate cancer patients did not worth the risk for expanding invasive prostate biopsy cases and medical costs. It was estimated that 5.2 million U.S. dollars would be spent for PSA screening to prevent one death from prostate cancer.[4] Therefore, a new biomarker set that can efficiently improve the poor specificity of PSA is urgently required for the reduction of risks above derived from overdiagnosis of prostate cancer.

Received: June 12, 2013
Published: August 30, 2013

dx.doi.org/10.1021/pr400547s | J. Proteome Res. 2013, 12, 4497−4506

Table 1. 116 Plasma Samples Used for Biomarker Screening

group	n		average age		gender
	screening set	validation set	screening set	validation set	
healthy controls	24	26	69.1	69.1	male
BPH[a]	19	19	68.9	68.9	male
PCa[b] (GS[c] 5–6)	20	17	65.3	65.9	male
PCa[b] (GS[c] 7)	28	30	69.7	64.2	male
PCa[b] (GS[c] 8–10)	25	18	68.1	66.1	male
total	116	110	68.2	64.0	male

[a]Benign prostate hypertrophy. [b]Prostate cancer. [c]Gleason score.

Various sophisticated proteomic techniques have been developed over a couple of decades to explore serum/plasma biomarkers. Most studies utilized focused proteomic technologies to reduce the complexity of serum/plasma proteome, targeting glycosylated proteins,[5,6] peptidome,[7,8] degradome,[9] or minor proteins.[10,11] Low-molecular-weight (LMW) proteome profiling methods have been also employed for biomarker discovery experiments to enrich and detect physiologically important polypeptides, such as cytokines, hormones, and antimicrobial peptides. Although previous LMW enrichment methods significantly enforced the detection limit of small polypeptides, it was difficult to guarantee throughput and reproducibility, which were essential for biomarker studies analyzing multiple clinical specimens.[12−15] For instance, size-exclusion chromatography on HPLC shows better reproducibility but lower throughput due to on-by-one injection of samples. Ultrafiltration spin cartridges show higher throughput but less reproducibility.

Therefore in this study we developed a novel LMW proteome-focusing technology that allows rapid, highly reproducible, and easy-to-operate enrichment of <20 kDa subproteome from crude plasma samples. The principle of this method was repeated purification of denatured undigested protein mixture on 96-well reversed phase chromatography plates. In the light of wide versatility, we named the method quick enrichment of small targets for mass spectrometry (QUEST-MS) technology. Here we applied QUEST-MS technology to both discovery phase and validation phase of prostate cancer biomarker development. Throughout the present study, we show a small neurotransmitter neuropeptide-Y (NPY) as a specific prostate cancer biomarker, which had potential to improve PSA test.

MATERIALS AND METHODS

Reagents

Tris(2-carboxyethyl)phosphine (TCEP), iodoacetamide, and ammonium bicarbonate were purchased from Sigma-Aldrich (Saint Louis, MO). Urea was purchased from GE Healthcare (Buckinghamshire, U.K.). Trypsin Gold was supplied by Promega (Madison, WI). Trifluoroacetic acid (TFA) was purchased from Shimadzu Corporation (Kyoto, Japan).

Plasma Samples

EDTA-plasma samples for biomarker screening (n = 116, Table 1) were collected in Kochi Medical School Hospital. For biomarker validation step, 40 healthy controls were collected in the Cancer Screening Center, The Cancer Institute Hospital of Japanese Foundation for Cancer Research (JFCR). Plasma samples from 20 benign prostate hyperplasia (BPH) patients and 65 prostate cancer patients were collected for validation study in Kochi Medical School Hospital, Kyoto University Hospital, and Iwate Medical University Hospital (Table 1). Plasma from prostate cancer patients and BPH patients were collected before any treatments. Healthy control samples were collected in conjunction with cancer screening. Plasma fraction was separated and stored in the standard operation procedure at hospitals. In brief, withdrawn blood was immediately mixed with EDTA-2K by converting container 10 times and subsequently centrifuged at 1100g for 10 min. The supernatant was aliquoted and stored at −80 °C until use. In all experiments plasma with a single freeze−thaw cycle were used. The research procedure was fully explained, and written informed consent was obtained from all of the patients above. This study was approved by individual institutional ethical committees: The Ethical Committee of RIKEN (Approval code: Yokohama H20-12 and H22-4), Institutional Review Board of Kochi Medical School, JFCR, Kyoto University, and Iwate Medical University.

QUEST-MS purification

On a 96-well polypropylene plate, 20 μL plasma samples were mixed with 80 μL of 10 M urea in 50 mM ammonium bicarbonate. After reduction with 5 mM TCEP at 37 °C for 15 min and alkylation with 25 mM iodoacetamide at room temperature for 15 min, samples were diluted four times with 50 mM ammonium bicarbonate and loaded onto equilibrated Oasis HLB 96-well μElution Plate (2 mg sorbent per well, 30 μm particle size, Waters Corporation, Milford, MA). Here all procedures on solid-phase extraction plates were performed with the custom-made 96-well syringe robot (Supplementary Figure S1 in the Supporting Information). The Oasis plate was prewetted with 500 μL of 70% acetonitrile and equilibrated with 500 μL of 0.1% TFA in 2% acetonitrile at 250 μL/min. Following sample loading at 100 μL/min, plates were washed twice with 500 μL of 0.1% TFA in 2% acetonitrile at 250 μL/min. Proteins were eluted with 100 μL of 40% acetonitrile at 100 μL/min and subsequently diluted five times with 0.1% TFA prior to second Oasis plate purification. The diluted samples were processed with the same conditions as those described in the first purification. The eluates were lyophilized by vacuum spin dryer, followed by digestion with 50 μL of 8 ng/μL Trypsin Gold (Promega) in 50 mM ammonium bicarbonate at 37 °C for 6 h. Digestive reaction was quenched by the addition of 50 μL 1.2% TFA in 4% acetonitrile.

LC/MS/MS Analysis

Following QUEST-MS purification above, 1 μL of sample was analyzed by LTQ-Orbitrap-Velos mass spectrometer (Thermo Fisher Scientific, Waltham, MA) equipped with Ultimate 3000 nanoflow HPLC (Thermo Fisher Scientific). Using 0.1% formic acid as Solvent A and 0.1% formic acid in acetonitrile as Solvent B, peptides were separated on C18 Chip-column (75 μm × 200 mm, Nikkyo Technos, Tokyo, Japan) by the gradient of Solvent B, 2 to 30% for 95 min and 30 to 95% for 15 min at the flow

dx.doi.org/10.1021/pr400547s | J. Proteome Res. 2013, 12, 4497−4506

rate 250 nL/min. The eluted peptides were ionized with the spray voltage 2000 V, and MS data were acquired in a data-dependent fragmentation method in which the survey scan was acquired between m/z 400 and 1600 at the resolution 60 000 with automatic gain control (AGC) target value of 1.0×10^6 ion counts. The top 20 intense precursor ions in each survey scan were subjected to low-resolution MS/MS acquisitions using normal CID scan mode with AGC target value of 5000 ion counts in the linear ion trap.

Label-Free Quantification on Expressionist RefinerMS

The raw data from LTQ-Orbitrap-Velos mass spectrometer were loaded onto Expressionist RefinerMS module (Genedata AG, Basel, Switzerland), which worked on the in-house server system for the subsequent data processing and label-free quantification analysis. The whole workflow of RefinerMS software is shown in Supplementary Figure S2 in the Supporting Information. After setting the Spectrum Grid at every 10 data points on 2D MS chromatogram planes ($x = m/z$ and y = RT), the first chemical noise subtraction was performed using RT Window = 500 scans and Quantile = 80. Following chromatogram smoothing by moving average estimator for every three RT scans in the second chemical noise subtraction, signals less than 1000 intensity were clipped in intensity thresholding. The third and fourth chemical noise subtractions were applied to data using RT structure removal at the minimum RT length = 8 scans and m/z structure removal at the minimum m/z length = 4 points, respectively. The chromatogram grid was set at every 10 scans on noise-subtracted data, followed by chromatogram RT alignment using parameters: m/z window =10 points, RT window =10 scans, gap penalty =1, RT search interval = 2 min, and alignment scheme = pairwise alignment-based tree. Next, the summed peak detection activity detected the peaks on a temporarily averaged chromatogram with parameters as follows: summation window = 2 min, overlap = 50, minimum peak size = 10 scans, maximum merge distance = 4 data points, gap/peak ratio = 10, method = curvature-based peak detection, peak refinement threshold = 5, and consistency filter threshold = 0.6. Finally summed isotope clustering activity grouped isotopic peaks derived from single molecule into an isotope cluster. Here parameters were used as follows: minimum charge = 1, maximum charge = 8, maximum missing peaks = 0, first allowed gap position = 3, ionization = protonation, RT tolerance = 0.1 min, m/z tolerance = 0.05 Da, and minimum cluster size ratio = 0.5.

Extraction of Biomarkers on Expressionist Analyst

Because the specificity of the new biomarker set should be maximized, 153 057 nonredundant detected peptides were filtered by Absent/Present Search algorithm that extracted peptides exhibiting all-or-nothing feature between two groups (healthy control + BPH vs prostate cancer). Peptides detected in at most 1 case among 43 controls and at least 11 cases among 73 prostate cancer patients were selected to be subjected to further validation experiments.

Protein Identification

The SEQUEST database search was performed on Proteome Discoverer 1.3 software (Thermo Fischer Scientific). The MS/MS data were searched against human protein database SwissProt 2012_09 (20 235 sequences) using search parameters as follows: enzyme name = trypsin, precursor mass tolerance = 3 ppm, fragment mass tolerance = 0.8 Da, dynamic modification = oxidation (M), and static modification = carbamidomethyl (C). We accepted peptide identifications that satisfied the false discovery rate (FDR) <1% by Peptide Validator activity in SEQUEST Decoy Database Search. The mass spectrometry proteomics data have been deposited to the ProteomeXchange Consortium (http://proteomecentral.proteomexchange.org) via the PRIDE partner repository with the data set identifier PXD000383 and DOI 10.6019/PXD000383.

Multiple Reaction Monitoring for NPY

Plasma samples were processed with QUEST-MS procedure as described above, except for the addition of final concentration 10 fmol/μL BSA tryptic digest as an internal control, prior to analysis by 4000 QTRAP mass spectrometer (AB Sciex, Foster City, CA) combined with Agilent 1200 nanoflow HPLC system (Agilent Technologies, Santa Clara, CA). Peptides were separated on C18 Chip-column (75 μm × 200 mm, Nikkyo Technos) using solvent A (0.1% formic acid) and solvent B (0.1% formic acid in acetonitrile). Two-step linear gradient of solvent B was configured from 2 to 30% for 10 min and from 30 to 95% for 5 min at flow rate of 250 nL/min. The multiple reaction monitoring (MRM) transitions specific to NPY and BSA (KYA technologies, Tokyo, Japan) were simultaneously monitored by the MRM mode in Analyst 1.5 software (AB Sciex, Foster City, CA). The instrumental settings were as follows: ionization spray voltage = 2200 V, curtain gas (N_2) = 12 psi, CAD = 4, declustering potential = 70 V, entrance potential = 10 V, Q1 resolution = HIGH, Q3 resolution = LOW, and pause in between = 2 ms. The acquired MRM chromatograms were analyzed with MultiQuant 2.02 software (AB Sciex, Foster City, CA). The mass chromatogram of each transition was smoothed by 1 pt window and quantified by peak area. After optimizing the collision energy (CE) for 12 NPY transitions, quantification was eventually performed using only Q1/Q3 = 466.23/272.20 corresponding to NPY_{81-88} peptide because this transition showed the highest sensitivity. Finally, area of NPY_{81-88} peak was normalized with equally spiked BSA digest as follows: normalized NPY = area (NPY_{81-88}, Q1/Q3 = 466.2/272.2)/area (BSA_{66-75}, Q1/Q3 = 582.3/951.5) × 10 000.

Silver Staining and Image Analysis

To evaluate the efficacy of QUEST-MS purification, we separated one-fifth of purified sample on 16% Tris-tricine SDS-PAGE gel (Life Technologies, Carlsbad, CA). The gel was stained with SilverQuest Silver Staining kit (Life Technologies) by following the manufacturer's instructions. Stained gel was scanned with a GS-800 calibrated densitometer (Bio-Rad Laboratories, Hercules, CA) and analyzed by Image J software.

Immunohistochemical Staining

Immunohistochemical study was carried out using the Ventana automated immunohistochemical systems (Ventana Medical Systems, Tucson, AZ). We used formalin-fixed and paraffin-embedded slice sections of surgical or biopsy specimens from the eight patients with prostate cancer. The eight prostate cancers included three with prostatic intraepithelial neoplasia (PIN) lesions. Sections were incubated with a 1:400 diluted solution of polyclonal anti-NPY antibody (Abcam, Cambridge, U.K.) for 16 min. The automated protocol was based on an indirect biotin−avidin system using a biotinylated universal secondary antibody and diaminobenzidine substrate with hematoxylin counterstaining. The specificity of the binding

dx.doi.org/10.1021/pr400547s | J. Proteome Res. 2013, 12, 4497−4506